Available online at www.sciencedirect.com
ScienceDirect
Journal of Organometallic Chemistry 692 (2007) 5605–5613
Journal of Organometallic Chemistry
www.elsevier.com/locate/jorganchem

Enolic Schiff-base aluminum complexes and their application in lactide polymerization

Xuan Pang [a,b], Xuesi Chen [a,*], Hongzhi Du [a,b], Xianhong Wang [a], Xiabin Jing [a]

[a] State Key Laboratory of Polymer Physics and Chemistry, Changchun Institute of Applied Chemistry, Chinese Academy of Sciences, Changchun 130022, PR China

[b] Graduate School of Chinese Academy of Sciences, Chinese Academy of Sciences, Beijing 100039, PR China

Received 17 July 2007; received in revised form 19 September 2007; accepted 20 September 2007

Abstract

A series of NNOO-tetradentate enolic Schiff-base ligands were prepared where ligand $\mathbf{L}_1$ = bis(benzoylacetone)propane-1,2-diimine, $\mathbf{L}_2$ = bis(acetylacetone)-propane-1,2-diimine, $\mathbf{L}_3$ = bis-(acetylacetone)cyclohexane-1,2-diimine. Their further reaction with aluminum tris(ethyl) formed complexes LAlEt (**1a**, **2a** and **3a)**. The solid structure of complexes **1a**, **2a** and **3a** confirmed by X-ray single crystal analysis manifested that these complexes were all monomeric and five-coordinated with an aluminum atom in the center. The configurations of these complexes varied from trigonal bipyramidal geometry (tbp) to square pyramidal geometry (sqp) due to their different auxiliary ligand architectures. ^{1}H NMR spectra indicated that all these complexes retained their configuration in solution states. Their catalytic properties to polymerize racemic-lactide (*rac*-LA) in the presence of 2-propanol were also studied. The diimine bridging parts as well as the diketone segment substituents had very close relationship with their performance upon the polymerization process. All these complexes gave moderately isotactic polylactides with controlled molecular weight and very narrow molecular weight distributions.

Keywords: Schiff base; Stereoselective; *rac*-Lactide

1. Introduction

Schiff bases and their metal complexes have been synthesized and characterized because Schiff bases are able to stabilize different metals in various oxidation states, controlling the performance of metals in a large variety of useful catalytic transformations [1]. Enolic Schiff-base ligands prepared from acetylacetone and related β-diketones with mono- or diamines have attracted much attention in recent years [2]. Because of their distinct advantages such as ease of synthesis, low cost as well as variety of coordination sites via different β-diketones and amines, they have been very important subject of coordination chemistry.

Biodegradable polyesters are prime biomedical materials as well as potential ecological thermoplastics that have gained increasing interest over the past decades [3]. These polymers are usually produced via the ring-opening polymerization (ROP) of cyclic esters. Polylactide (PLA) is one of the most important biodegradable polyesters [4]. Because lactides have three different stereoisomers (Scheme 1), their polymers may have different chain configurations. The physical and mechanical properties of PLAs, as well as their rate of degradation, are intimately dependent on the chain stereochemistry [5]. A stereocomplex polymer formed by an equivalent mixture of poly(L-lactide) (PLLA) and poly(D-lactide) (PDLA) has many advantages such as higher melting temperature (230 °C) comparing with the enantiopure polylactide (180 °C) [6]. So the direct ring-opening polymerization (ROP) of racemic-lactide (*rac*-LA) (*rac*-LA is a 1:1 mixture of L-LA and D-LA) via the stereoselective catalysts become significative challenges and opportunities

* Corresponding author. Tel./fax: +86 431 85262112.
E-mail address: xschen@ciac.jl.cn (X. Chen).

0022-328X/$ - see front matter © 2007 Elsevier B.V. All rights reserved.
doi:10.1016/j.jorganchem.2007.09.014

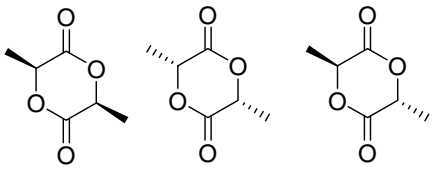

Scheme 1. Stereoisomers of lactides.

for chemists. In 1993, Spassky et al. reported a Schiff-base aluminum complex to polymerize *rac*-LA in toluene at 70 °C to moderately isotactic polymer [7]. Recently, many excellent catalysts were synthesized to polymerize *rac*-LA in a stereoselective manner [8]. To better explore the potential applications of enolic Schiff-base ligands as metal-chelating agents and their further use as precursors in the cyclic ester polymerization, we have prepared three NNOO-tetradentate enolic Schiff-base ligands and their aluminum complexes. In this paper, we reported the synthesis, characterization of the three momomeric Schiff-base aluminum complexes, their polymeric performance were also discussed in detail.

2. Result and discussion

2.1. Complex formation and complexes structure characterization

Ligands $\mathbf{L}_1$, $\mathbf{L}_2$ and $\mathbf{L}_3$ were easily synthesized from readily available starting materials, namely primary diamines, 1-benzoylacetone and acetylacetone. Reaction of ligands $\mathbf{L}_1$, $\mathbf{L}_2$ and $\mathbf{L}_3$ with $AlEt_3$ in toluene at 80 °C formed complexes **1a**, **2a** and **3a**, respectively. Complexes **1a** and **2a** had identical diimine bridging parts but different enol substituents: phenyl for complex **1a** and methyl for complex **2a**; while complexes **2a** and **3a** had same enol structure but different diimine bridging parts: propane-1,2-diimine for complex **2a** and cyclohexane-1,2-diimine for complex **3a**.

Table 1
Selected bond distances (Å) and angles (°) for **1a**

Al–N(1)	1.982(2)	Al–N(2)	2.0144(18)
Al–O(1)	1.8469(15)	Al–O(2)	1.8197(17)
Al–C(24)	1.982(2)		
O(2)–Al–O(1)	87.71(7)	O(2)–Al–C(24)	110.08(10)
O(1)–Al–C(24)	98.17(8)	O(2)–Al–N(1)	127.90(8)
O(1)–Al–N(1)	89.22(7)	C(24)–Al–N(1)	121.83(10)
O(2)–Al–N(2)	88.13(8)	O(1)–Al–N(2)	162.99(8)
C(24)–Al–N(2)	98.75(9)	N(1)–Al–N(2)	80.38(8)

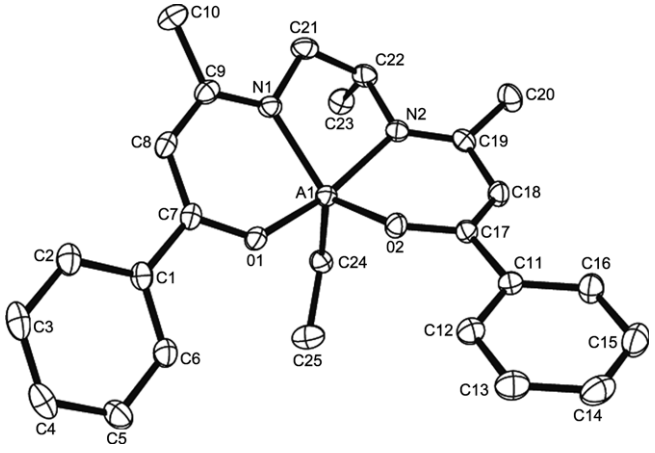

Fig. 1. Molecular structure of **1a**.

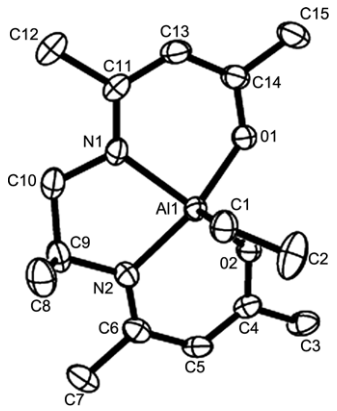

Fig. 2. Molecular structure of **2a**.

Table 2
Selected bond distances (Å) and angles (°) for **2a**

Al–N(1)	1.984(3)	Al–N(2)	2.013(3)
Al–O(1)	1.851(3)	Al–O(2)	1.835(3)
Al–C(1)	1.970(4)		
O(2)–Al–O(1)	83.83(11)	O(2)–Al–C(1)	110.02(15)
O(1)–Al–C(1)	102.26(16)	O(2)–Al–N(1)	142.18(13)
O(1)–Al–N(1)	88.45(12)	C(1)–Al–N(1)	107.80(16)
O(2)–Al–N(2)	88.16(12)	O(1)–Al–N(2)	150.57(14)
C(1)–Al–N(2)	107.08(16)	N(1)–Al–N(2)	80.69(13)

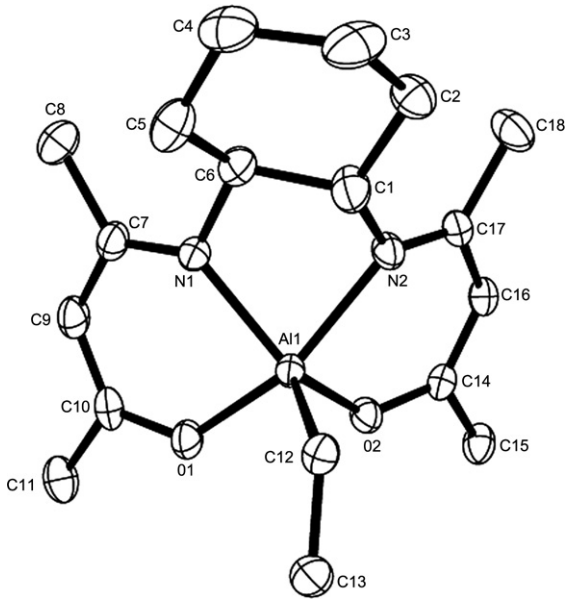

Fig. 3. Molecular structure of **3a**.

Single crystal analysis of **1a** showed that **1a** was monomeric with a five-coordinated aluminum atom in the center. The geometry around the Al atom was trigonal bipyramidal geometry with an average compressed axial O(1)–Al(1)–N(2) bond angle of 162.99(8)°, and equatorial O(2)–Al–N(1), C(24)–Al–N(1), and O(2)–Al–C(24) bond angles of 127.90(8)°, 121.83(10)°, and 110.08(10)°, respectively. Central Al atom is ca. 0.55 Å above the N(1)N(2)C(24) mean plane in the direction of O(1). The distances from the Al atom to O(1), O(2), N(1), N(2) and C(24) were 1.8469(15), 1.8197(17), 1.982(2), 2.0144(18) and 1.982(2) Å, respectively (Table 1). The molecular structure of **1a** was shown in Fig. 1. The molecular structure of **2a** was shown in Fig. 2. The geometry around the Al atom was distorted square pyramidal with the ethyl group lying on the axial position and two nitrogen atoms and two oxygen atoms on the basal position. Central Al atom is ca. 0.55 Å above the N(1)N(2)O(1)O(2) mean plane with an average compressed axial O(1)–Al(1)–N(2) bond angle of 150.57(14)° and equatorial O(2)–Al–N(1), C(1)–Al–N(1), and O(2)–Al–C(1) bond angles of 142.18(13)°, 107.80(16)°, and 110.02(15)°, respectively. The distances from the Al(1) atom to O(1), O(2), N(1), N(2) and C(1) were 1.851(3), 1.835(3), 1.984(3), 2.013(3), and 1.970(4) Å, respectively (Table 2). X-ray single crystal structure analysis of **3a** also showed a five-coordination around the aluminum center (Fig. 3). The geometry around the Al atom was a distorted square pyramidal with the ethyl group lying on the axial position and two nitrogen atoms and two oxygen atoms on the basal position. Central Al atom is ca. 0.07 Å above the N(1)N(2)O(1)O(2) mean plane with an average compressed axial O(1)–Al(1)–N(2) bond angle of 155.48 (10)° and equatorial O(2)–Al(1)–N(1), N(1)–Al(1)–C(12) and O(2)–Al(1)–C(12) bond angles of 136.78(10)°, 113.16(11)° and 109.67(11)°, respectively. The distances from the Al atom to O(1), O(2), N(1), N(2) and C(12) were 1.8491(19), 1.8251(19), 1.994(2), 2.037(2) and 1.996(3) Å, respectively (Table 3). The crystallographic data of complexes **1a**, **2a** and **3a** were listed in Table 4.

The Al–C bond lengths of complexes **1a** and **2a** were 1.982 Å (**1a**) and 1.970 Å (**2a**), respectively. We presumed that the longer Al–C bond in **1a** was due to the conjugated

Table 3
Selected bond distances (Å) and angles (°) for **3a**

Al–N(1)	1.994(2)	Al–N(2)	2.037(2)
Al–O(1)	1.8491(19)	Al–O(2)	1.8251(19)
Al–C(12)	1.996(3)		
O(2)–Al–O(1)	87.60(9)	O(2)–Al–C(12)	109.67(11)
O(1)–Al–C(12)	102.97(11)	O(2)–Al–N(1)	136.78(10)
O(1)–Al–N(1)	88.29(9)	C(12)–Al–N(1)	113.16(11)
O(2)–Al–N(2)	88.68(9)	O(1)–Al–N(2)	155.48(10)
C(12)–Al–N(2)	101.10(11)	N(1)–Al–N(2)	77.98(9)

Table 4
Crystallographic data for **1a**, **2a** and **3a**

Complex	**1a**	**2a**	**3a**
Empirical formula	$C_{25}H_{29}AlN_2O_2$	$C_{15}H_{25}AlN_2O_2$	$C_{18}H_{29}AlN_2O_2$
Formula weight	416.48	292.35	332.41
Temperature (K)	187(2)	187.0(2)	187(2)
Wavelength (Å)	0.71073	0.71073	0.71073
Crystal system	Triclinic	Monoclinic	Monoclinic
Space group	$P\bar{1}$	$P2_1/n$	$P2_1/n$
a (Å)	10.7131(10)	17.883(2)	8.1424(8)
b (Å)	10.8103(10)	13.4216(16)	13.4924(14)
c (Å)	11.2956(11)	14.9483(19)	16.8954(18)
α (°)	80.759(2)	90	90
β (°)	70.655(2)	114.035(2)	102.170(2)
γ (°)	64.820(2)	90	90
Volume (Å^3)	1116.72	3276.7(7)	1814.4(3)
Z	2	8	4
D_{calc} (Mg m^{-3})	1.239	1.185	1.217
Absorption coefficient (mm^{-1})	0.114	0.127	0.123
F(000)	444	1264	720
Crystal size (mm)	$0.17 \times 0.11 \times 0.09$	$0.43 \times 0.33 \times 0.16$	$0.38 \times 0.18 \times 0.12$
θ Range (°)	1.91–26.03	1.96–25.58	1.95–26.03
Limiting indices (hkl range)	$-13 \leqslant h \leqslant 1$, $-13 \leqslant k \leqslant 9$, $-13 \leqslant l \leqslant 13$	$-21 \leqslant h \leqslant 19$, $-16 \leqslant k \leqslant 15$, $-10 \leqslant l \leqslant 18$	$-4 \leqslant h \leqslant 10$, $-16 \leqslant k \leqslant 16$, $-20 \leqslant l \leqslant 18$
Reflections collected	6260	17 120	9958
Independent reflections	4299	6130	3555
R_{int}	0.0227	0.0488	0.0242
Goodness-of-fit on F^2	1.017	1.018	1.029
Final R_1, wR_2 [$I > 2\sigma(I)$]	0.0546, 0.1183	0.0794, 0.1822	0.0640, 0.1667
R_1, wR_2 (all data)	0.0813, 0.1322	0.1083, 0.2013	0.0755, 0.1775
Largest difference in peak and hole (e Å^{-3})	0.282 and −0.202	0.758 and −0.687	1.013 and −0.437

Table 5
Polymerization data of *rac*-LA using **1a**, **2a** and **3a** in toluene at 70 °C[a]

Entry	Complex	$[LA]_0/[Al]/[^iPrOH]$	Time (h)	Conversion[b] (%)	M_n (calculated)	M_n^c (GPC)	M_n^d	*Pm*[e]	PDI[c]
1	**1a**	35/1/1	31	93	4.7	7.8	4.55	0.77	1.02
2[f]	**1a**	35/1/1	8	90	4.5	7.4	4.30	0.73	1.23
3[g]	**1a**	35/1/1	2.5	91	4.6	7.0	4.05	0.71	1.29
4	**1a**	40/1/1	32	90	5.2	9.3	5.38	0.74	1.05
5	**2a**	22/1/1	24.8	88	2.8	5.7	3.28	0.72	1.03
6	**2a**	42/1/1	27	90	5.5	8.8	5.08	0.72	1.05
7	**2a**	57/1/1	50	85	6.6	11.9	6.89	0.73	1.06
8	**3a**	72/1/1	41.5	86	8.9	17.2	10	0.65	1.25
9	**3a**	100/1/1	32	63	9.0	17.3	9.86	0.65	1.28
10	**3a**	100/1/2	32	65	4.5	8.6	5.0	0.65	1.22
11	**3a**	100/1/4	32	62	2.2	4.5	2.6	0.65	1.22

[a] All reactions performed with $[LA]_0 = 0.48$ mol L^{-1}.
[b] Measured by ^1H NMR.
[c] Determined from GPC and calibrated by PS standard.
[d] Calculated from the value of M_n determined by GPC according to formula $M_n = 0.58 M_n(GPC)$ [10].
[e] *Pm* is the probability of *meso* linkages [12].
[f] Reaction at 90 °C.
[g] Reaction at 110 °C.

effect of the phenyl substituent in the enol segment. Comparing with **2a**, the Al–C bond length of complex **3a** (1.996 Å) was much longer, indicating a weaker bond. The difference in the bond lengths between **2a** and **3a** resulted from the different bridging parts they contained. We hypothesized that the shorter bond length was resulted from the weaker steric repulsion between the bridging part and ethyl group in **2a**. To figure out whether these complexes retained their monomeric structures as they had in solution state, we investigated the ^1H and ^{27}Al NMR spectra of these complexes. The ^1H NMR spectra of **1a**–**3a** showed one set of resonance peak and the ^{27}Al NMR spectra of **1a**–**3a** showed resonance peak at about 32 ppm, indicating that all the ethyl complexes retained their conformation with the five-coordinated monomeric Al center in the solution states [9].

2.2. Polymerization

Complexes **1a**, **2a** and **3a** were used as precursors in the racemic-lactide polymerization to examine the influence of different diimine bridging parts and enol substituents on their catalytic performance, respectively. The polymerization results were collected in Table 5. The polymerization process was investigated by kinetic studies. The data of conversions vs. time were collected in Figs. 4–6. First-order kinetics in monomer was observed in all cases. The number-average molecular weight (M_n) also followed a linear relationship in monomer conversion (Fig. 7). All the three complexes provided the characteristic features of the living propagation as it was seen in the linear correlations between M_n and conversion, linear semi-logarithmic kinetic dependencies (Figs. 4–6), as well as by the low polydispersities less than 1.1. The apparent polymerization rate constant (k_{app}) were obtained from these figures. The k_{app} values for **1a**, **2a** and **3a** were 0.085 h^{-1} (Table 5, entry 1), 0.047 h^{-1} (Table 5, entry 6) and 0.046 h^{-1} (Table 5, entry 8), respectively. The polymerization rate constants (k_p) could be calculated from the equation $k_p = k_{app}/[Al]$ correspondingly. The k_p values for **1a**, **2a** and **3a** were 5.95 L mol^{-1} h^{-1}, 3.87 L mol^{-1} h^{-1} and 6.56 L mol^{-1} h^{-1}, respectively. To determine the order in Al, k_{app} was plotted vs. the concentration of Al using **2a** (Fig. 8). From this plot, k_{app} increased linearly with the increasing of the Al

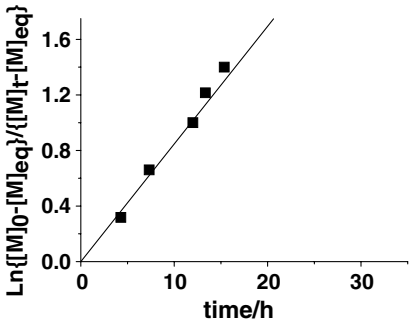

Fig. 4. Kinetic plots of the *rac*-lactide conversion with the reaction time using **1a**/2-propanol, [LA]/[Al] = 35.

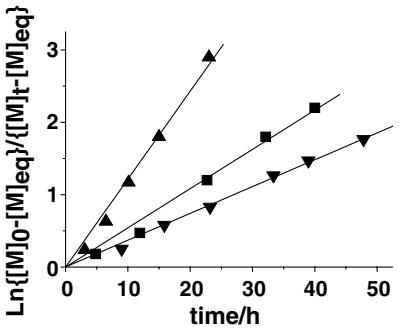

Fig. 5. Kinetic plots of *rac*-lactide conversion with reaction time using **2a**/2-propanol: (▲) [LA]/[Al] = 22, (■) [LA]/[Al] = 42, and (▼) [LA]/[Al] = 57.

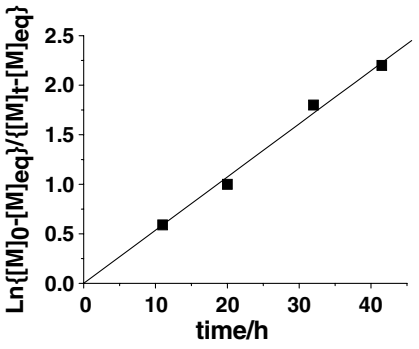

Fig. 6. Kinetic plots of *rac*-lactide conversion with reaction time using **3a**/2-propanol, [LA]/[Al] = 72.

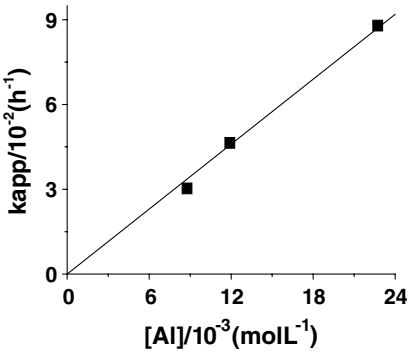

Fig. 8. k_{app} with the concentration of the **2a**/2-propanol initiator for the *rac*-LA polymerization.

concentration, indicating that the order in Al was first order. Therefore, the polymerization of *rac*-LA using **2a** followed an overall kinetic equation:

$$-\mathrm{d}[\mathrm{LA}]/\mathrm{d}t = k_{\mathrm{p}}[\mathrm{LA}][\mathrm{Al}].$$

Complex **3a** had the longest Al–C bond among the three complex, Lin et al. [11] reported that the stronger the metal–alkoxide bond, the slower the reaction time. It was hypothesized that complex that containing the weaker Al–C bonds (longer bond length) was easier to cleave when coordinated with the incoming monomer. So the complex would have higher activity. Complex **3a** which containing the longest Al–C bond had the highest activity (Table 5, entry 9). Complexes **1a** and **2a** had identical diimine bridging part but different enol substituents. Comparing with **2a**, **1a** with the phenyl group has slightly higher activity. Complexes **2a** and **3a** had identical enol structure but different diimine bridging parts. Complex **2a** had higher stereoselectivity but lower activity than **3a**. It was postulated that the more rigid diimine bridging part in **3a** could not offer enough steric hindrance; it made the incoming monomer easier to insert and coordinate with the Al center. The homonuclear decoupled ^{1}H NMR spectrum in the methine region of polylactide samples by **1a** manifested the polymer chain were most predominantly isotactic (Fig. 9) and the *Pm* value was 0.77 [12]. Recently, some interesting work [13] reported that in the presence of an excess of 2-propanol, polymers with narrow polydispersities and controlled molecular weights, which could be predicted from the monomer/alcohol ratio were formed via alcohol exchange. These catalytic systems showed the "immortal" character. To explore the potential "immortal" character of our

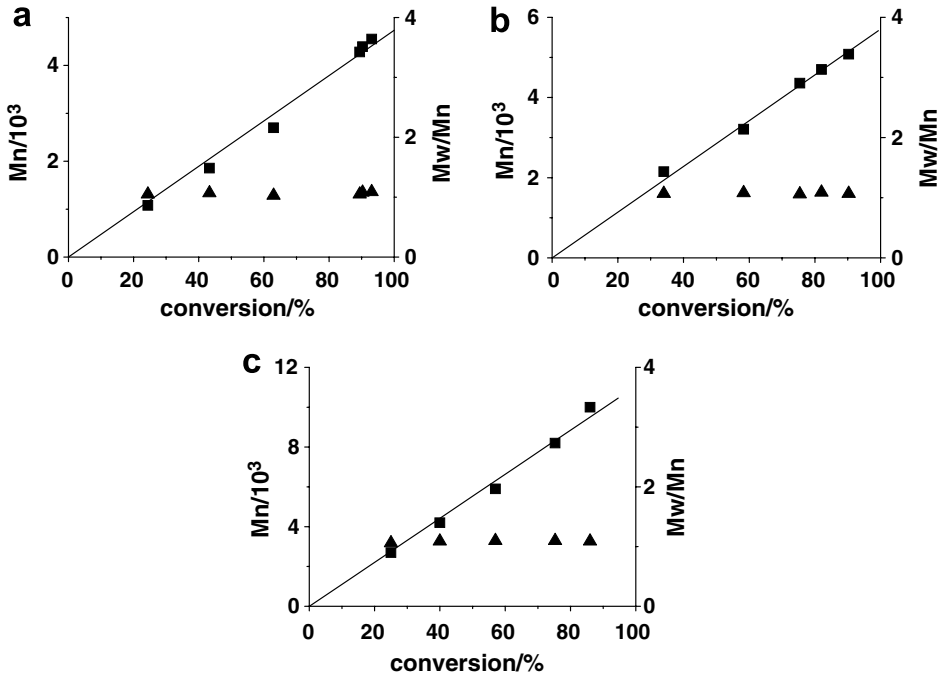

Fig. 7. Plot of PLA M_n and polydispersity (M_w/M_n) as a function of *rac*-lactide conversion using (a) complex **1a**/2-propanol, [LA]/[Al] = 35; (b) complex **2a**/2-propanol, [LA]/[Al] = 42, and (c) complex **3a**/2-propanol, [LA]/[Al] = 72.

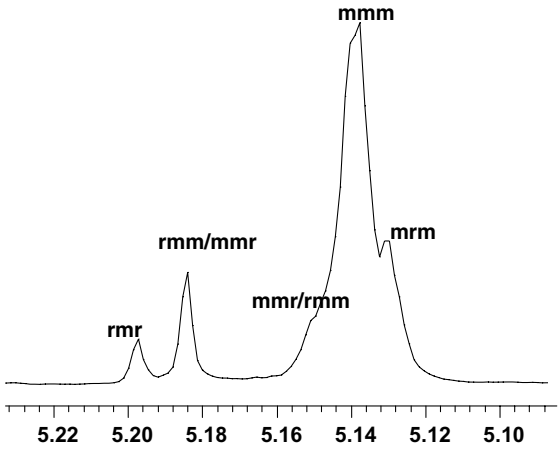

Fig. 9. Methine region of homonuclear decoupled ^{1}H NMR spectrum of poly(*rac*-LA) using **1a**.

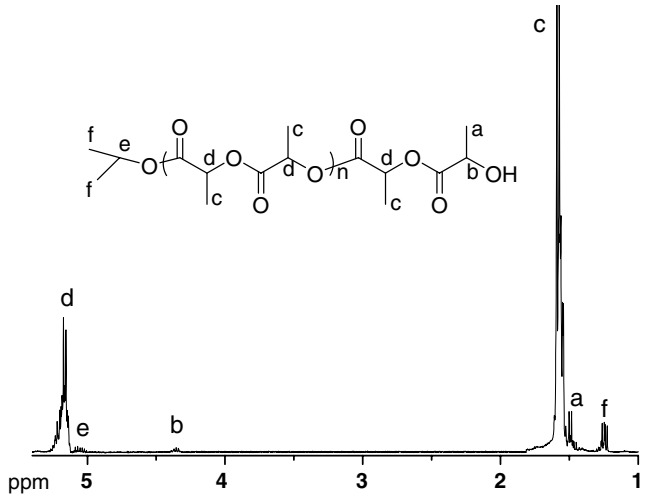

Fig. 10. ^{1}H NMR spectrum of oligomers of *rac*-LA in $CDCl_3$.

catalytic system, we have investigated the polymerization of *rac*-LA with different [2-propanol]/[**3a**], the results manifested that **3a** was active in the "immortal" polymerization. There was a linear relationship between the M_n values of the PLA and the 2-propanol added. In fact, the M_n values increased proportionally to the amount of 2-propanol added and the polydispersities were still very low (Table 5, entries 10 and 11).

The influence of temperature on the polymerization rate was also investigated using **1a**/2-propanol. The stereoselectivity decreased with the increasing temperature, while the polymerization rate increased. The *Pm* values and the apparent polymerization rate constants (k_{app}), the polymerization rate constants (k_p) at the different temperatures were collected in Table 6. The activation energy of the polymerization was calculated by fitting these values contained in Table 3 to the Arrhenius equation ($k_p = A e^{-Ea/RT}$). A value of 68.6 kJ mol^{-1} for the activation energy was deduced by means of an adequate representation of $\ln k_p$ vs. $1/T$.

The ^{1}H NMR spectrum of the LA oligomers (Fig. 10) prepared with a molar ratio of [*rac*-LA]:[**1a**]:[2-propanol] = 10:1:1 after quenching with a little acetic acid in 5 h showed that the integral ratio of the two peaks at 1.24 ppm (the methyl protons of the isopropoxycarbonyl end group) and 4.35 ppm (the methine proton neighboring the hydroxyl end group) was close to 6:1. This indicated that the polymer chains were end-capped with an isopropyl ester and a hydroxyl group [14] and the ring-opening occurred through a so-called coordination-insertion mechanism [15].

Table 6
Kinetic results of *rac*-LA polymerization at different temperature using **1a**

T (°C)	k_{app} (h^{-1})	k_p (L mol^{-1} h^{-1})	*Pm*
70	0.085	5.95	0.77
90	0.32	22.4	0.73
110	1.60	112	0.71

3. Conclusion

Three enolic Schiff-base aluminum complexes derived from β-diketone and diamine were synthesized. Single crystal data manifested that all these complexes had five-coordination around the aluminum center. Complex **3a** which containing the longest Al–C bond had the highest activity in the ROP of *rac*-lactide polymerization. These complexes polymerized lactides in good controlled manner and in some cases affording moderately isotactic polylactide (complexes **1a** and **2a**). Their different performances in the *rac*-LA polymerization were due to their different diimine bridging parts and substituent groups in the enol segment. First-order kinetics in both monomer and initiator were observed.

4. Experimental

4.1. General

All experiments were carried out under argon using Schlenk techniques. Starting materials for the synthesis of ligands $\mathbf{L}_1$, $\mathbf{L}_2$ and $\mathbf{L}_3$ were purchased from Aldrich Inc. and used without further purification. Chiral diamines were used as racemates. All solvents were purified from a Mbraun SPS system. Racemic-lactide (Purac) was purified by recrystallization from ethyl acetate and dried under vacuum at room temperature before use. NMR spectra were recorded on Bruker AV 400 M in $CDCl_3$ at 25 °C. Chemical shifts were given in parts per million from tetramethylsilane. Gel permeation chromatography (GPC) measurements were conducted with a Waters 515 GPC with $CHCl_3$ as the eluent (flow rate: 1 mL min^{-1}, at 35 °C). The molecular weights were calibrated against polystyrene (PS) standards. Crystallographic data were collected on a Bruker APEX CCD diffractometer with graphite-monochromated Mo Kα radiation ($\lambda = 0.71073$ Å) at 187 K. The structure was refined by the full-matrix least-

squares method on F^2 using the SHELXTL-97 crystallographic software package. Anisotropic thermal parameters were used to refine all nonhydrogen atoms. Hydrogen atoms were located in idealized positions. Crystals suitable for X-ray diffraction were grown from a mixture of toluene and hexane at −10 °C. The crystallographic data and the results of refinements were summarized in Table 1.

4.2. Ligand synthesis

General procedure. A solution of diamine (0.1 mol L^{-1}) in ethanol (50 mL) was added dropwise to a stirred solution of β-diketone (0.2 mol L^{-1}) in ethanol (100 mL). The reaction mixture was refluxed for 10 h before cooling to room temperature. After removal of the solvent under vacuum, a crystalline solid was produced and purified by recrystallization in ethanol (Scheme 2).

*Ligand **L**$_1$*. Ligand $\mathbf{L}_1$ was obtained as a white crystalline solid in 85% yield. ^{1}H NMR (400 M, $CDCl_3$): δ 7.86 (d, 4H, Ar*H*), 7.42 (m, 6H, Ar*H*), 5.70 (b, 2H, C*H*COH), 3.93 (m, 1H, (CH_3)C*H*N), 3.48 (m, 2H, CH_2N), 2.09 (d, 6H, CH_3C=N), 1.42 (d, 3H, (CH_3)CHN) ppm. ^{13}C NMR (100 M, $CDCl_3$): δ 187.0 (Ar*C*OH), 163.9, 163.2 (CH_3*C*=N), 139.1, 129.6, 127.2, 125.9 (Ar*C*), 91.8 (*C*HCOH), 49.2 ((CH_3)*C*HN), 48.8 (*C*H_2N), 18.5 (*C*H_3C=N), 18.1 ((*C*H_3)CHN) ppm. Elemental Anal. Calc. for $\mathbf{L}_1$: C, 76.21; H, 7.23; N, 7.73. Found: C, 76.10; H, 7.21; N, 7.60%.

*Ligand **L**$_2$*. Ligand $\mathbf{L}_2$ was obtained as a white crystalline solid in 83% yield. ^{1}H NMR (400 M, $CDCl_3$): δ 5.01 (b, 2H, C*H*COH), 3.75 (m, 1H, (CH_3)C*H*N), 3.34 (t, 2H, CH_2N), 2.03 (s, 6H, CH_3COH), 1.91 (d, 6H, CH_3C=N), 1.32(d, 3H, (CH_3)CHN) ppm. ^{13}C NMR (100 M, $CDCl_3$): δ 194.8 (CH_3*C*OH), 162.7, 162.0 (CH_3*C*=N), 95.7 (*C*HCOH), 49.5 ((CH_3)*C*HN), 49.3 (*C*H_2N), 28.6 (*C*H_3COH), 19.3 (*C*H_3C=N), 18.4 ((*C*H_3)CHN) ppm. Elemental Anal. Calc. for $\mathbf{L}_2$: C, 65.51; H, 9.30; N, 11.75. Found: C, 65.30; H, 10.05; N, 11.68%.

*Ligand **L**$_3$*. Ligand $\mathbf{L}_3$ was obtained as a yellow crystalline solid in 87% yield. ^{1}H NMR (400 M, $CDCl_3$): δ 5.17 (s, 2H, C*H*COH), 3.22 (t, 2H, C*H*), 2.06 (b, 4H, cyclohexane H), 2.00 (s, 6H, CH_3COH), 1.84 (s, 6H, CH_3C=N), 1.45 (m, 2H, cyclohexane H), 1.28(m, 2H, cyclohexane H) ppm. ^{13}C NMR (100 M, $CDCl_3$): δ 195.2 (CH_3*C*OH), 163.1 (CH_3*C*=N), 95.7 (*C*HCOH), 58.0 (cyclohexane C), 33.3 (cyclohexane C), 29.1 (*C*H_3COH), 24.8 (*C*H_3C=N), 19.0 (cyclohexane C) ppm. Elemental Anal. Calc. for $\mathbf{L}_3$: C, 69.03; H, 9.41; N, 10.06. Found: C, 69.42; H, 9.25; N, 10.31%.

4.3. Complex synthesis

General procedure. $AlEt_3$ (0.2 mmol, 0.023 g) in toluene (5 mL) was added to the stirred toluene solution (3 mL) of ligand (0.2 mmol) at room temperature (RT). The reaction was maintained at 80 °C for 12 h, the reaction mixture was then slowly cooled to RT (Scheme 3). The toluene was removed under vacuum.

*Complex **1a***. Complex **1a** was obtained as a yellow solid in 87% yield. ^{1}H NMR (400 M, $CDCl_3$): δ 8.00 (m, 4H, Ar*H*), 7.40 (m, 6H, Ar*H*), 5.86 (s, 1H, C*H*COAl), 5.81 (s, 1H, C*H*COAl), 4.05 (m, 1H, (CH_3)C*H*N), 3.51 (m, 1H,

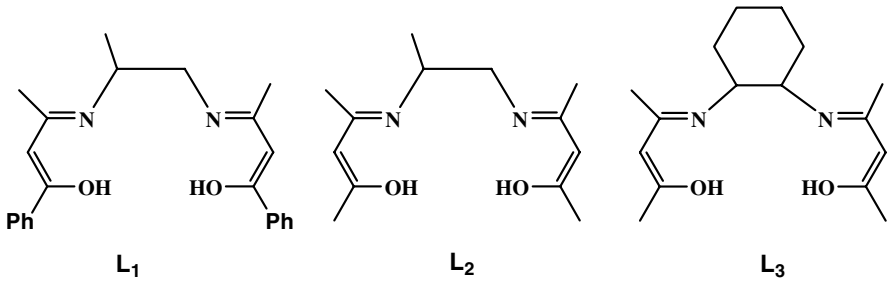

Scheme 2. Ligands prepared in this paper.

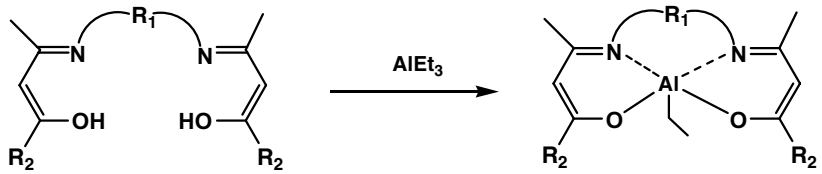

1a: R_1= -CH(CH_3)CH_2-, R_2=Ph;
2a: R_1= -CH(CH_3)CH_2-, R_2=CH_3;
3a: R_1= -CH(CH_2)$_4$CH-, R_2=Ph.

Scheme 3. Synthetic pathway for preparation of **1a**, **2a** and **3a**.

CH_2N), 3.46 (m, 1H, CH_2N), 2.21 (s, 3H, $CH_3C{=}N$), 2.19 (s, 3H, $CH_3C{=}N$), 1.36 (d, 3H, $(CH_3)CHN$), 0.89 (t, 3H, $AlCH_2CH_3$), −0.30 (q, 2H, $AlCH_2CH_3$) ppm. ^{13}C NMR (100 M, $CDCl_3$): δ 174.9, 174.5 (Ar*C*OAl), 173.0, 170.6 ($CH_3C{=}N$), 139.4, 130.5, 128.6, 127.5 (Ar*C*), 97.6, 97.1 (*C*HCOAl), 54.1 ($(CH_3)CHN$), 52.4 (CH_2N), 23.8 ($CH_3C{=}N$), 22.6 ($(CH_3)CHN$) 20.5 ($AlCH_2CH_3$), 10.6 ($AlCH_2CH_3$) ppm. Elemental Anal. Calc. for **1a**: C, 72.09; H, 7.02; N, 6.73. Found: C, 71.77; H, 7.05; N, 6.55%.

*Complex **2a***. Complex **2a** was obtained as a yellow solid in 79% yield. ^1H NMR (400 M, $CDCl_3$): δ 5.12 (s, 1H, C*H*COAl), 5.02 (s, 1H, C*H*COAl), 3.91(m, 1H, $(CH_3)CHN$), 3.32 (t, 2H, CH_2N), 2.02 (s, 3H, CH_3COAl), 2.00 (s, 3H, CH_3COAl), 1.97 (d, 6H, $CH_3C{=}N$), 1.26 (d, 3H), 0.93 (t, 3H, $AlCH_2CH_3$), −0.39 (q, 2H, $AlCH_2CH_3$) ppm. ^{13}C NMR (100 M, $CDCl_3$): δ 181.0, 179.2 (CH_3COAl), 173.7, 170.0 ($CH_3C{=}N$), 99.7, 99.2 (*C*HCOAl), 53.4 ($(CH_3)CHN$), 51.6 (CH_2N), 25.83 (CH_3COAl), 22.7 ($CH_3C{=}N$), 20.7 ($(CH_3)CHN$), 14.1 ($AlCH_2CH_3$), 9.8 ($AlCH_2CH_3$) ppm. Elemental Anal. Calc. for **2a**: C, 61.62; H, 8.62; N, 9.58. Found: C, 61.20; H, 8.34; N, 9.83%.

*Complex **3a***. Complex **3a** was obtained as a yellow solid in 82% yield. ^1H NMR (400 M, $CDCl_3$): δ 5.05 (s, 1H, C*H*COAl), 4.79 (s, 1H, C*H*COAl), 3.82 (m, 1H, C*H*), 3.07 (t, 1H, C*H*), 2.49 (b, 1H, cyclohexane H), 2.10 (b, 1H, cyclohexane H), 2.02 (s, 3H, CH_3COAl), 1.98 (s, 3H, CH_3COAl), 1.89 (s, 6H, $CH_3C{=}N$), 1.80 (m, 2H, cyclohexane H), 1.40 (m, 4H, cyclohexane H), 0.92 (t, 3H, $AlCH_2CH_3$), −0.17 (q, 2H, $AlCH_2CH_3$) ppm. ^{13}C NMR (100 M, $CDCl_3$): δ 181.0, 176.4 (CH_3COAl), 165.6, 162.7 ($CH_3C{=}N$), 101.1, 99.0 (*C*HCOAl), 63.4, 57.7, 33.7, 33.0 (cyclohexane C), 28.8, 26.7 (CH_3COAl), 25.7, 25.6 ($CH_3C{=}N$), 24.6, 24.4 (cyclohexane C) 18.7 ($AlCH_2CH_3$), 10.0 ($AlCH_2CH_3$) ppm. Elemental Anal. Calc. for **3a**: C, 65.04; H, 8.79; N, 8.43. Found: C, 64.83; H, 8.96; N, 8.75%.

4.4. Polymerization of rac-LA

General procedure. Under the protection of argon, the *rac*-LA (2.24 mmol, 0.323 g), 2-propanol (0.06 mmol, in 0.5 mL of toluene), complex (**1a**, **2a** or **3a**) (0.06 mmol in 0.2 mL of toluene), and toluene (3.8 mL) were added to a dried reaction vessel equipped with a magnetic stirring bar, respectively. The vessel was placed in an oil bath at 70 °C. Conversion of the monomer was determined on the basis of ^1H NMR spectroscopic studies. The polymers were isolated by precipitation into cold methanol, then filtrated and dried under vacuum at room temperature for 24 h.

5. Supplementary material

CCDC 290873, 654187 and 654188 contain the supplementary crystallographic data for **1a**, **2a** and **3a**. These data can be obtained free of charge from The Cambridge Crystallographic Data Centre via www.ccdc.cam.ac.uk/data_request/cif.

Acknowledgements

This project is financially supported by the National Natural Science Foundation of China (Project No. 20574066) and National Fund for Distinguished Young Scholar (No. 50425309).

References

[1] R.A. Sheldon, J.K. Kochi, in: Metal Catalysed Oxidations of Organic Compounds, Academic Press, New York, 1981, pp. 97, 102 and 105.
[2] For recent reviews, see: (a) L. Canali, D. Sherrington, Chem. Soc. Rev. 28 (1999) 85;
(b) J. Severn, J. Chadwick, R. Duchateau, Nic. Friederichs, Chem. Rev. 105 (2005) 4073.
[3] (a) K.E. Uhrich, S.M. Cannizzaro, R.S. Langer, K.M. Shakesheff, Chem. Rev. 99 (1999) 3181;
(b) D.J. Mooney, G. Organ, J.P. Vacanti, R. Langer, Cell Transplant. 2 (1994) 203;
(c) J.L. Eguiburu, M.J. Fernandez-Berridi, F.P. Cossio, J. San Roman, Macromolecules 32 (1999) 8252;
(d) A.-C. Albertsson, I.K. Varma, Biomacromolecules 4 (2003) 1466;
(e) B.J. O'Keefe, M.A. Hillmyer, W.B. Tolman, J. Chem. Soc., Dalton Trans. (2001) 2215;
(f) Z.Y. Zhong, P.J. Dijkstra, C. Birg, M. Westerhausen, J. Feijen, Macromolecules 34 (2001) 3863;
(g) D. Takeuchi, T. Nakamura, T. Aida, Macromolecules 33 (2000) 729;
(h) B.J. O'Keefe, L.E. Breyfogle, M.A. Hillmyer, W.B. Tolman, J. Am. Chem. Soc. 124 (2002) 4384.
[4] (a) R.E. Drumright, P.R. Gruber, D.E. Henton, Adv. Mater. 12 (2000) 1841;
(b) E. Chiellini, R. Solaro, Adv. Mater. 8 (1996) 305.
[5] (a) M.S. Reeve, S.P. McCarthy, M.J. Downey, R.A. Gross, Macromolecules 27 (1994) 825;
(b) J.R. Sarasua, R.E. Prud'homme, M. Wisniewski, A. LeBorgne, N. Spassky, Macromolecules 31 (1998) 3895.
[6] (a) Y. Ikada, K. Jamshidi, H. Tsuji, S.H. Hyon, Macromolecules 20 (1987) 904;
(b) H. Tsuji, Y. Ikada, Polymer 40 (1999) 6699.
[7] A. LeBorgne, V. Vincens, M. Jouglard, N. Spassky, Makromol. Chem. Macromol. Symp. 73 (1993) 37.
[8] (a) T.M. Ovitt, G.W. Coates, J. Am. Chem. Soc. 124 (2002) 1316;
(b) C.P. Radano, G.L. Baker, M.R. Smith, J. Am. Chem. Soc. 122 (2000) 1552;
(c) Z.Y. Zhong, P.J. Dijkstra, J. Feijen, Angew. Chem. 114 (2002) 4692;
Z.Y. Zhong, P.J. Dijkstra, J. Feijen, Angew. Chem., Int. Ed. 41 (2002) 4510;
(d) Z.Y. Zhong, P.J. Dijkstra, J. Feijen, J. Am. Chem. Soc. 125 (2003) 11291;
(e) N. Nomura, R. Ishii, M. Akakura, K. Aoi, J. Am. Chem. Soc. 124 (2002) 5938;
(f) M. Wisniewski, A. LeBorgne, N. Spassky, Macromol. Chem. Phys. 198 (1997) 1227;
(g) Z.H. Tang, X.S. Chen, Y.K. Yang, X. Pang, J.R. Sun, X.F. Zhang, X.B. Jing, J. Polym. Sci. A 42 (2004) 5974;
(h) Z.H. Tang, X.S. Chen, X. Pang, Y.K. Yang, X.F. Zhang, X.B. Jing, Biomacromolecules 5 (2004) 965;
(i) H.Y. Ma, G. Melillo, L. Oliva, T.P. Spaniol, U. Englert, J. Okuda, Dalton Trans. (2005) 721;
(j) K. Majerska, A. Duda, J. Am. Chem. Soc. 126 (2004) 1026;

(k) P. Hormnirun, E.L. Marshall, V.C. Gibson, A.J.P. White, D.J. Williams, J. Am. Chem. Soc. 126 (2004) 2688;
(l) R. Ishii, N. Nomura, T. Kondo, Polym. J. 36 (2004) 261.
[9] R. Benn, A. Rufinska, H. Lemkuhl, E. Janssen, C. Kruger, Angew. Chem., Int. Ed. Engl. 22 (1983) 779.
[10] (a) T. Biela, A. Duda, S. Penczek, Macromol. Symp. 183 (2002) 1;
(b) M. Save, M. Schappacher, A. Soum, Macromol. Chem. Phys. 203 (2002) 889;
(c) A. Duda, A. Kowalski, S. Penczek, Macromolecules 31 (1998) 2114;
(d) S.J. McLain, N.E. Drysdale, Polym. Prepr. 33 (1992) 463;
(e) J. Baran, A. Duda, A. Kowalski, R. Szymanski, S. Penczek, Macromol. Rapid Commun. 18 (1997) 325;
(f) A. Duda, S. Penczek, Macromolecules 23 (1990) 1636.
[11] H.Y. Chen, H.Y. Tang, C.C. Lin, Macromolecules 39 (2006) 3745.
[12] *Pm* is the probability of *meso* linkages, $[\mathrm{mmm}] = Pm^2 + (1 - Pm)Pm/2$, $[\mathrm{mmr}] = [\mathrm{rmm}] = (1 - Pm)Pm/2$, $[\mathrm{rmr}] = (1 - Pm)^2/2$, $[\mathrm{mrm}] = [(1 - Pm)^2 + Pm(1 - Pm)]/2$.
[13] (a) T. Aida, Y. Maekawa, S. Asano, S. Inoue, Macromolecules 21 (1988) 1195;
(b) E. Martin, P. Dubois, R. Je'rôme, Macromolecules 33 (2000) 1530;
(c) A. Amgoune, C.M. Thomas, J.F. Carpentier, Macromol. Rapid Commun. 28 (2007) 693.
[14] Z.Y. Zhong, P.J. Dijkstra, C. Birg, M. Westerhausen, J. Feijen, Macromolecules 34 (2001) 3863.
[15] (a) H.R. Kricheldorf, S.R. Lee, S. Bush, Macromolecules 29 (1996) 1375;
(b) W.M. Stevels, P.J. Dijkstra, J. Feijen, Trends Polym. Sci. 5 (1997) 300;
(c) P. Dubois, C. Jacobs, R. Jerome, P. Tessie, Macromolecules 24 (1991) 2266;
(d) A. Kowalski, A. Duda, S. Penczek, Macromolecules 31 (1998) 2114;
(e) A. Kowalski, A. Duda, S. Penczek, Macromolecules 33 (2000) 689.